2026 IEEE 23rd Consumer Communications & Networking Conference (CCNC), 9-12 January 2026, Las Vegas, NV, USA
DOI: 10.1109/CCNC65079.2026.11366517

Industrial Case Study of Aerial Systems Using Ray-Tracing and Antenna Optimisation

Krishnakanth Mohanta
Faculty of Engineering & Applied Sciences
Cranfield University, United Kingdom
krishnakanth.mohanta.012@cranfield.ac.uk

Saba Al-Rubaye
Faculty of Engineering & Applied Sciences
Cranfield University, United Kingdom
s.alrubaye@cranfield.ac.uk

Antonios Tsourdos
Faculty of Engineering & Applied Sciences
Cranfield University,United Kingdom
a.tsourdos@cranfield.ac.uk

***Abstract*—An industrial case study of Unmanned Aerial System (UAS) operation and communications for integrated satellite-terrestrial networks in remote regions is considered. The objective is to evaluate and optimize the Quality of Service (QoS) of communication networks that combine satellite backhaul and ground-based transmission infrastructure for UAS operations. To address this challenge, this paper proposes a new algorithm for antenna tilt optimization procedure aiming to enhance terrestrial coverage, and maximise average Received Signal Strength Indicator (RSSI) along predefined UAS paths using terrain-aware ray-tracing models. A preliminary analysis of the satellite link is performed using simulation-based model of phased array terminal, assessing its suitability for Beyond Visual Line of Sight (BVLOS) operations through latency and RSSI profiling under variable link conditions. In addition, the study quantifies the QoS of the terrestrial network by analyzing RSSI, Signal-to-Interference-plus-Noise Ratio (SINR), latency, and throughput across UAS routes between key islands. The findings highlight the effectiveness of hybrid satellite-terrestrial architectures in extending coverage and reliability for critical UAS operations in geographically challenging environments. This work informs future network planning strategies for remote UAS deployments.**

***Index Terms*—UAV Communications, Satellite-Terrestrial Integration, Quality of Service (QoS), Ray-Tracing Propagation Modelling, Antenna Optimisation**

I. Introduction

Unmanned Aerial Systems (UAS) are becoming increasingly vital in addressing challenges related to logistics, surveillance, emergency response, and infrastructure inspection in remote and sparsely connected regions. Ensuring continuous and reliable communication links for UAS operations in these environments is critical for enabling Beyond Visual Line of Sight (BVLOS) missions [1] and maintaining Command and Control (C2), telemetry, and high-throughput data flows [2], [3]. The fifth generation (5G) cellular technology is a key enabler of these use cases [4]–[7]. The proposed hybrid architecture is shown in Figure 1, in which a 5G terrestrial access link is backhauled via a Low Earth Orbit (LEO) satellite constellation. While terrestrial 5G coverage can be sparse or absent on remote islands, space-based connectivity offers scalable, low-latency backhaul for UAS operations [8]. Recent advances in phased-array antennas for LEO and high-altitude platforms (HAPs) further enable dynamic links that support UAS mobility [9]. Moreover, integration of satellite communications (SATCOM) with 5G enhances reliability, ensuring uninterrupted service where ground networks alone would fail [10], [11]. Although this work employs a 5G network architecture and LEO satellites, lessons may be drawn from 6G and other heterogeneous frameworks [12]–[18].

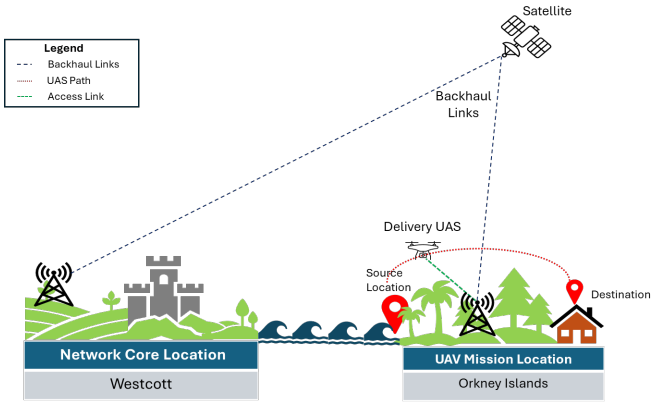

Fig. 1. Network Architecture for UAS BVLOS operations

This paper focuses on hybrid communication architecture that leverages both terrestrial networks and satellite links to support UAS operations across key routes in the remote region. The Orkney Islands, taken as a use case for this study is a remote archipelago off the northern coast of Scotland, present a compelling testbed for such operations due to their rugged topography, variable weather, and limited terrestrial infrastructure. It investigates three interrelated objectives: (i) a preliminary QoS analysis of the satellite backhaul link, (ii) to develop an algorithm for antenna angle optimisation to maximise Received Signal Strength Indicator (RSSI) along UAS trajectories, and (iii) detailed modelling of terrestrial network performance, including RSSI, SINR, throughput, latency and spatial coverage.

The remainder of this paper is structured as follows. Section II presented the System design and hybrid satellite–terrestrial architecture. Section III provides analysis of the Satellite Backhaul, Terrestrial Network Analysis with antenna operatisation is presented in Section IV. Finally, Section V summarising key findings.

Published by IEEE. This is the Author Accepted Manuscript issued with: Creative Commons Attribution License (CC:BY 4.0).
The final published version (version of record) is available online at DOI:10.1109/CCNC65079.2026.11366517. Please refer to any applicable publisher terms of use.

II. System Design

This section outlines the methodology used to model and optimise a hybrid satellite-terrestrial communication system for UAS operations in remote rural regions. It covers (i) the test-site and data preparation, (ii) the system architecture, and (iii) QoS metrics and modelling techniques forming the basis for subsequent analysis.

A. Test Site Definition

The Orkney Islands comprise over 70 islands off Scotland's northern coast, characterised by rugged terrain and sparse infrastructure. Three representative islands: Stromness, Hoy, and Graemsay were selected owing to their varied topography and existing Royal Mail UAS routes. Digital Elevation Models (DEM) and OpenStreetMap (OSM) building data were integrated within a geographic information system (GIS) to generate accurate terrain profiles along predefined UAS trajectories at 85 m altitude. These data enabled ray-tracing simulations to capture line-of-sight (LOS) conditions, diffraction, and multipath effects over both land and sea. The test site and antenna locations are shown in Fig. 2.

Fig. 2. Remote Test Site Definition (Orkney)

B. Communication System Architecture

The hybrid architecture (Fig. 1) comprises two segments: (i) a *satellite backhaul* using a Ku-band LEO constellation with a phased-array ground terminal, modelled using publicly available Starlink parameters, and (ii) a *terrestrial 5G network* with two fixed base stations at Stromness and Hoy operating at 3.5 GHz and 40 dBm transmit power. The Stromness antenna, mounted 15 m above ground, employs a 65° beamwidth MIMO panel antenna. Both stations connect via the satellite backhaul to a central core in Westcott.

C. QoS Metrics and Modelling Techniques

Four primary QoS metrics are used as the key performance indicators (KPIs) in this study: RSSI, SINR, latency, and throughput.

1) **RSSI:** Computed from the link budget [26]:

$$RSSI = P_{Tx} + G_{Tx} + G_{Rx} - L_{path} - L_{misc} \quad (1)$$

where P_{Tx}, G_{Tx}, and G_{Rx} denote transmit power and antenna gains; L_{path} is path loss from ray-tracing; and L_{misc} includes system and atmospheric losses. RSSI was sampled along each UAS path for both satellite and terrestrial links.

2) **SINR:** For the terrestrial network, co-channel interference between transmitters is modelled as:

$$SINR = \frac{P_{signal}}{P_{interference} + P_{noise}} \quad (2)$$

with noise power $N = kTB$, where k is Boltzmann's constant, T is noise temperature, and $B = 100$ MHz is the noise bandwidth.

3) **Latency:** Propagation delay for satellite links includes uplink and downlink paths plus a 6 ms processing delay, while the terrestrial round-trip latency accounts for ray-traced path length and a 2 ms processing delay at each 5G node.

4) **Throughput:** Derived from local SINR via spectral-efficiency mapping:

$$T(x_m, y_m) = \eta(SINR(x_m, y_m)) \times B_{\text{eff}} \quad (3)$$

where $\eta(SINR)$ is obtained from SINR-MCS lookup tables (e.g., 5G NR) and B_{eff} denotes usable bandwidth. The same approach applies for Ku-band NTN links.

III. Preliminary Analysis of Satellite Backhaul

The satellite backhaul employs the Starlink LEO constellation operating in the Ku-band. Orbital elements were obtained from publicly available Two-Line Element (TLE) sets [23] and propagated to determine satellite elevation and azimuth as viewed from the ground terminals at Stromness and Hoy.

A. LEO Satellite and Ground-Terminal Modelling

Satellite and ground-terminal characteristics were modelled using FCC filings and open-source specifications. Although hardware details may vary slightly, parameters such as transmit power, gain, and losses were selected from reliable literature to maintain realistic link budgets [19]. The main parameters used for system simulation are summarised in Tables I and II.

TABLE I
Satellite Antenna Characteristics

Parameter	Satellite Tx	Satellite Rx
Downlink frequency (GHz)	10.7-12.7	-
Uplink frequency (GHz)	-	14-14.5
Max. EIRP (dBW)	66.9	-
Gain (min-max, dBi)	34.5-44.5	34.5-44.5
Losses (dB)	0.5	0.5

TABLE II
STARLINK GROUND TERMINAL CHARACTERISTICS

Parameter	Value
Rx gain (downlink)	35.8 dBi
Tx gain (uplink)	37.2 dBi
Gain at max. slant (Tx/Rx)	32.2 / 31.5 dBi
Peak Tx power (per beam)	4.06 W
Max. EIRP (uplink)	38.2 dBW
Uplink / Downlink bands (GHz)	14-14.5 / 10.7-12.7
Modulation	Up to 64-QAM
Implementation loss	0.5 dB

B. Link Budget Computation

A simulation was performed over a one-hour window using the parameters in Tables I-II. Coaxial cable losses (15 m) between the ground terminal and tower were included. Figure 3 shows the simulated RSSI for both the gateway-to-satellite and satellite-to-tower links.

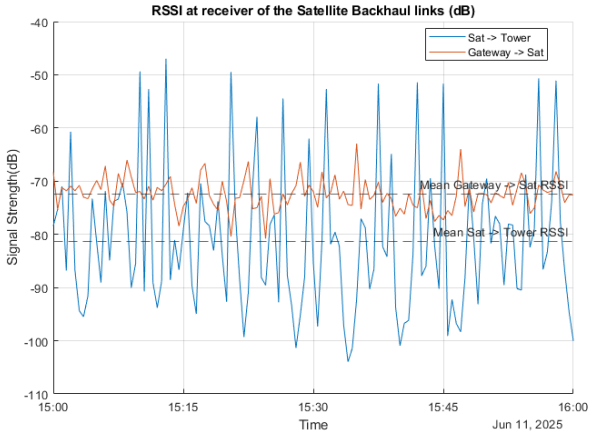

Fig. 3. RSSI at the Stromness tower (blue) and satellite terminal (red)

The uplink (Gateway → Satellite) RSSI remains between -69 dB and -75 dB (mean ≈ -72 dB), while the downlink (Satellite → Tower) averages -82 dB with brief fades below -100 dB at low elevation angles, still above the receiver sensitivity of -119 dB. A 5 dB rain-fade margin ensures link reliability even during adverse weather. The results confirm that the high-gain terminals sustain near-continuous connectivity despite horizon loss and terrain diffraction effects. Figure 4 presents the corresponding one-way link latencies. The Gateway → Satellite delay ranges between 10.4-11.2 ms (mean 10.6 ms), and Satellite → Tower latency varies from 12.0-13.4 ms (mean 12.5 ms), reflecting slant-range variation during orbital passes.

Overall, the combined round-trip latency of the Ku-band backhaul remains below 25 ms, comfortably within the 50 ms threshold for real-time BVLOS command-and-control operations.

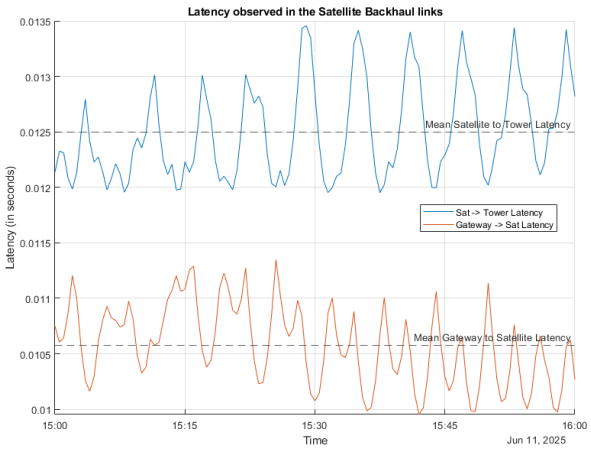

Fig. 4. Latency in the satellite backhaul links

IV. TERRESTRIAL NETWORK ANALYSIS

Ensuring robust terrestrial connectivity for UAS operations in the Orkney Islands requires careful design of ground-station transmissions over highly irregular terrain. In our scenario, a single directional transmitter (Tx_1) must simultaneously serve two fixed UAS trajectories, one over Graemsay and one over Hoy, without relocating the antenna or altering its power. The only controllable parameter is the azimuth angle of Tx_1. If this angle is chosen poorly, portions of one or both paths may fall below the receiver sensitivity threshold (-100 dBm), jeopardising command-and-control, telemetry and video links. The use of terrain-aware ray-tracing models and digital elevation maps enables a realistic representation of signal propagation over a rural landscape [20], [21]. Moreover, the inclusion of OpenStreetMap (OSM) building data and local topographic relief enhances the fidelity of site-specific performance predictions. Since simple free-space model cannot capture the effect of terrain, 3D ray-tracing was employed. This allows to account for LOS blockages, diffraction over hills and reflections from water and stone structures. The difference between the RSSI calculated by the raytracing model and the freespace model can be seen in Figure 5.

Without these terrain-induced variations, free-space models would underestimate worst-case losses by up to 20 dB, risking coverage gaps if antenna angles were not optimised. The parameters used for the raytracing are tabulated in Table III.

The antenna characteristics for the base stations are listed in Table IV. A panel antenna is used at Graemsay for providing connectivity to both the UAS paths. An isotropic antenna is installed at Hoy to provide connectivity close to the Hoy island. The UAS paths are defined with waypoints. The Graemsay UAS path has 76 waypoints, whereas the Hoy UAS path has 58 waypoints.

A. Transmitter Angle Optimisation

In the scenario shown in Figure 2, UAS trajectories and transmitter locations are fixed, leaving only the azimuth angle

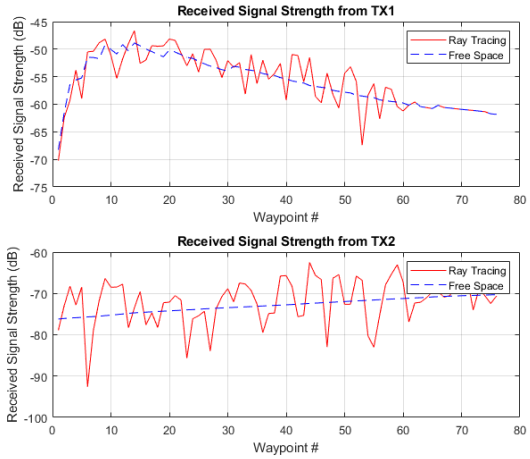

Fig. 5. Received Signal Strength Raytracing model vs Freespace model

TABLE III
RAY-TRACING SIMULATION PARAMETERS

Parameter	Value
Building conductivity, σ_{build}	0.02 S/m
Building relative permittivity, $\epsilon_{r,build}$	5
Ground conductivity, σ_{ground}	0.01 S/m
Ground relative permittivity, $\epsilon_{r,ground}$	15
Seawater conductivity, σ_{sea}	4.64 S/m
Seawater relative permittivity, $\epsilon_{r,sea}$	81
Diffractions considered	Yes
Reflections considered	Yes
Maximum number of reflections	5

of Tx_1 adjustable. The received power must stay above the receiver sensitivity of -100 dBm at all waypoints to maintain reliable command, telemetry, and video links. Manual inspection alone cannot determine the optimal balance, hence an optimisation process is required.

Optimising the antenna angle ensures all waypoints exceed -100 dBm while maximising average RSSI. The analysis iterates over candidate angles $\Theta = \{-90°, -100°, \ldots, -160°\}$, invoking ray-tracing at each Θ and selecting the angle giving the highest mean RSS across both trajectories:

$$J(\Theta) = \frac{1}{N_1 + N_2}\Big(\sum_{w \in P_1} RSSI(w, \Theta) + \sum_{v \in P_2} RSSI(v, \Theta) \Big)$$

Here N_1 and N_2 are waypoint counts on Graemsay and Hoy paths, respectively. $RSSI(x, \phi)$ is the received signal (dBm) at waypoint x for azimuth ϕ, and $J(\Theta)$ is the mean RSSI for both paths. Algorithm 1 outlines the optimisation logic. In this study, RSSI is prioritised, though other metrics (e.g., SNR, throughput) can be incorporated via weighting.

Table V lists mean RSSI for each angle. The optimal $\Theta = -110°$ achieves the highest overall mean (-53.75 dBm) with all waypoints above -100 dBm. This angle is used for subsequent terrestrial QoS analysis.

TABLE IV
GROUND ANTENNA PARAMETERS FOR TERRESTRIAL TRANSMITTERS

Parameter	Tx1/Rx1 AW3923	Tx2/Rx2 Isotropic
Antenna type	4×4 MIMO	Ideal isotropic
Frequency of operation	3.5 GHz	3.5 GHz
Transmit power	40 dBm	40 dBm
Antenna gain (boresight)	18 dBi	3 dBi

Algorithm 1 Tx_1 Antenna Angle Optimisation

Require: $P_1 = \{w_1, \ldots, w_{N_1}\}$ (Graemsay), $P_2 = \{v_1, \ldots, v_{N_2}\}$ (Hoy)
Require: E (3D environment), Tx_2 (fixed site), f (3.5 GHz), PATTERN (Tx_1 pattern)
Require: $\Theta = \{-90°, -100°, \ldots, -160°\}$, S (sensitivity, -100 dBm)
Ensure: θ^* (optimal Tx_1 azimuth)
Initialise ray-tracing model $M \leftarrow (E, f, \text{PATTERN}, \ldots)$
$R \leftarrow \varnothing$ ▷ feasible angles with scores
for $\theta \in \Theta$ **do**
  Configure Tx_1 at azimuth θ
  $r_1 \leftarrow [\text{RayTraceRSS}(Tx_1, Tx_2, w, M) \ : \ w \in P_1]$
  $r_2 \leftarrow [\text{RayTraceRSS}(Tx_1, Tx_2, v, M) \ : \ v \in P_2]$
  if $\min(r_1) \geq S$ **and** $\min(r_2) \geq S$ **then**
    $\mu_{\text{avg}} \leftarrow (\text{mean}(r_1) + \text{mean}(r_2))/2$
    $R \leftarrow R \cup \{(\theta, \mu_{\text{avg}})\}$
  end if
end for
if $R \neq \varnothing$ **then**
  $\theta^* \leftarrow \arg\max_{(\theta,\mu) \in R} \ \mu$
  return θ^*
else
  report "No feasible angle"
  return $\theta^* = \text{NaN}$
end if

TABLE V
MEAN RSS ALONG UAS PATHS AT DIFFERENT Tx_1 ANGLES.

Antenna Angle	Graemsay (dBm)	Hoy (dBm)	Overall Mean (dBm)
-90	-53.065	-57.220	-55.143
-100	-52.525	-55.902	-54.214
-110	-52.500	-54.991	-53.745
-120	-53.036	-54.516	-53.776
-130	-54.094	-54.418	-54.256
-140	-55.726	-54.719	-55.222
-150	-57.901	-55.320	-56.611
-160	-60.545	-56.179	-58.362

B. Terrestrial Network Simulation and Analysis

With Tx_1 fixed at the optimised azimuth $\Theta = -110°$, ray-tracing was executed using the settings in Table III. The model coherently sums all ray components to compute QoS at the receiver. The same process was applied to both UAS trajectories, and the resulting metrics are summarised below.

1) **RSSI:** All waypoints exceed -100 dBm, with an overall mean of -53.75 dBm. The combined RSS for both routes, accounting for best-server handovers, is shown

in Figure 6, indicating consistent link quality along both flight paths.

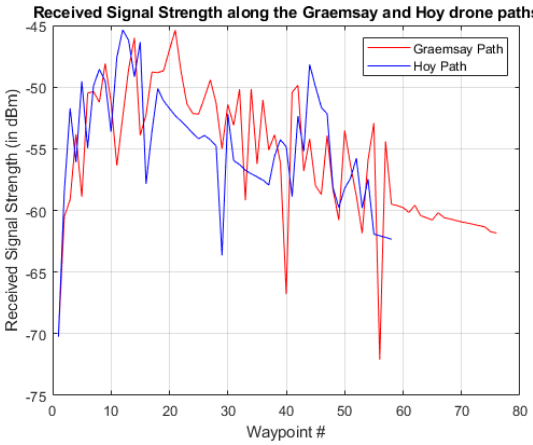

Fig. 6. RSSI comparison between Graemsay and Hoy UAS paths.

2) **SINR:** Treating TX_1 and TX_2 as co-channel interferers, SINR was computed at each waypoint using the ray-tracing model. Results are shown in Figure 7.

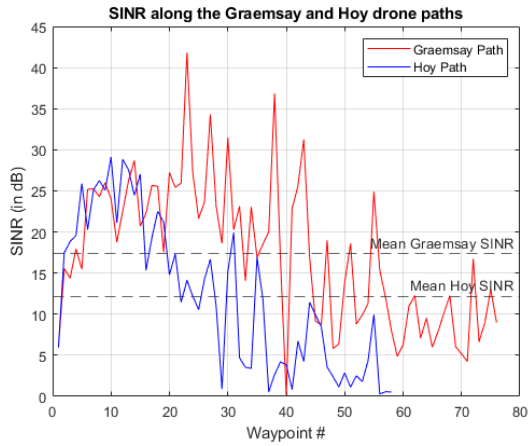

Fig. 7. SINR variation along Graemsay and Hoy UAS paths.

On the Graemsay route, SINR stays mostly above 10 dB, peaking near 40 dB (waypoint 22) with a brief dip to 0.1 dB (waypoint 40); mean SINR = 17.33 dB. On the Hoy route, SINR averages 12.12 dB, typically above 10 dB with occasional 0-2 dB dips due to terrain-induced diffraction. Overall, the optimised azimuth provides stable SINR coverage above 0 dB along both routes, confirming robust connectivity.

3) **Throughput:** Algorithm 2 shows the calculation of throughput using SINR–CQI mapping. SINR samples were mapped via standard SINR→CQI→MCS conversion using predefined 5G NR parameters specified in [27]. Throughput assumptions are in Table VI.
Figure 8 shows per-waypoint throughput: Graemsay reaches up to 35 Mbps at high CQIs before dropping below 6 Mbps beyond waypoint 40. Hoy maintains high throughput up to waypoint 25, dips near waypoint 30, and declines after waypoint 50. Both routes sustain at least 6 Mbps-adequate for real-time C2, telemetry, and video transmission in Orkney's terrain.

Algorithm 2 Per-Waypoint Throughput Calculation (CQI→MCS Mapping)

Require: $\text{sinr1}[1..N_1][1..2]$ ▷ Graemsay waypoints (Tx_1, Tx_2)
Require: $\text{sinr2}[1..N_2][1..2]$ ▷ Hoy waypoints (Tx_1, Tx_2)
Require: $\text{mcsTable}[1..15, 4]$ ▷ [$SINR_{thres}$, CQI, modOrder, codeRate×1024]
Require: maxPRBs, SCS_kHz
Ensure: $T1[1..N_1]$, $T2[1..N_2]$ ▷ Throughput per waypoint (bps)

$\text{codeRate}[i] \leftarrow \text{mcsTable}[i, 4]/1024$
$\text{symbolsPerPRB} \leftarrow 12 \times (\text{SCS_kHz}/15)$
function COMPUTETHROUGHPUT($\text{sinr}[], N$)
  for $t = 1$ to N **do**
    $s \leftarrow \max(\text{sinr}[t, 1], \text{sinr}[t, 2])$ ▷ Best server SINR
    $\text{idx} \leftarrow \max\{i : \text{mcsTable}[i, 1] \leq s\}$
    if idx empty **then**
      $T[t] \leftarrow 0$
    else
      $(m, cr) \leftarrow (\text{mcsTable}[idx, 3], \text{codeRate}[idx])$
      $bitsPRB \leftarrow \text{symbolsPerPRB} \times \log_2(m) \times cr$
      $T[t] \leftarrow bitsPRB \times \text{maxPRBs}$
    end if
  end for
  return T
end function
$T1 \leftarrow$ COMPUTETHROUGHPUT($\text{sinr1}, N_1$) ▷ Graemsay
$T2 \leftarrow$ COMPUTETHROUGHPUT($\text{sinr2}, N_2$) ▷ Hoy

TABLE VI
KEY ASSUMPTIONS FOR THROUGHPUT CALCULATION

Parameter	Value / Assumption
Subcarrier spacing (SCS)	30 kHz
PRB bandwidth	$12 \times \text{SCS} = 360$ kHz
Usable system bandwidth	100 MHz × 0.9864 = 98.64 MHz
Maximum PRBs	$\left\lfloor \frac{98\,640 \text{ kHz}}{360 \text{ kHz}} \right\rfloor = 274$
Symbols per PRB	S_{PRB} =12 × $\frac{\text{SCS}}{15 \text{ kHz}} = 12$
Bits per PRB calculation	$S_{PRB} \times \log_2$(modOrder) × codeRate
Throughput per waypoint (bps)	T (bps) = bitsPerPRB × maxPRBs
Conversion to Mbps	Mbps = $\frac{T(bps)}{10^6}$

V. CONCLUSION

This study demonstrated the feasibility of a hybrid satellite-terrestrial communication network for BVLOS UAS operations in the Orkney Islands. QoS analysis of the Ku-band Starlink backhaul showed stable gateway-to-satellite performance (RSSI ≈ -72 dB, latency ≈ 10.6 ms) and a mean satellite-to-tower RSSI of -82 dB with brief fades at low elevation angles (latency ≈ 12.5 ms). On the terrestrial side, raytracing

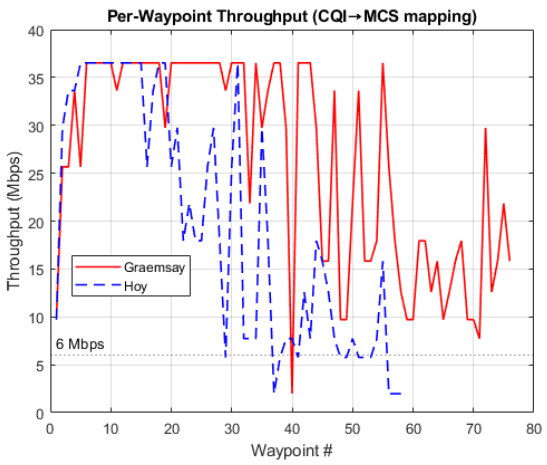

Fig. 8. Throughput (Mbps) along Graemsay (red) and Hoy (blue) paths

over terrain and building data revealed up to 20 dB variation in path loss compared to free-space estimates. Optimising the Stromness transmitter azimuth ($-110°$) ensured full waypoint coverage above the sensitivity limit, while 5G NR SINR-CQI-MCS throughput mapping confirmed sustained rates above 6 Mbps, sufficient for command, telemetry, and video on both Graemsay and Hoy routes. Overall, the combination of a high-gain LEO backhaul and optimised ground-station alignment achieves low-latency, high-throughput links suitable for BVLOS operations in challenging island terrain. Though the simulation model is validated at Westcott test data, future work will focus on field validation, adaptive beam-steering, integration of HAP relays for multi-link diversity, and machine-learning-based optimisation of antenna orientation and flight paths to enhance reliability in rural UAS deployments.

ACKNOWLEDGMENT

This work is supported by Connectivity for Remote Orkney Future Transport (CROFT) project, which is funded by the European Space Agency (ESA) under the Advanced Research in Telecommunications Systems (ARTES) program. The authors express their gratitude to the project consortium, led by industrial partners Skyports, Satellite Applications Catapult, WM5G, and Stratospheric Platforms Ltd.

REFERENCES

[1] Mousa, M. & Al-Rubaye, S. Intelligent 5G-Aided UAV Positioning in High-Density Environments Using Neural Networks for NLOS Mitigation. *Aerospace*. **12** (2025), https://www.mdpi.com/2226-4310/12/6/543

[2] Warrier, A., Aljaburi, L., Whitworth, H., Al-Rubaye, S. & Tsourdos, A. Future 6G Communications Powering Vertical Handover in Non-Terrestrial Networks. *IEEE Access*. **12** pp. 33016-33034 (2024)

[3] Whitworth, H., Al-Rubaye, S. & Tsourdos, A. Utilizing Satellite Communication to Enable Robust Future Flight Data Links. *2023 IEEE/AIAA 42nd Digital Avionics Systems Conference (DASC)*. pp. 1-8 (2023)

[4] Ullah, H., Gopalakrishnan Nair, N., Moore, A., Nugent, C., Muschamp, P. & Cuevas, M. 5G communication: An overview of vehicle-to-everything, drones, and healthcare use-cases. *IEEE Access*. **7** pp. 37251-37268 (2019)

[5] Kumar, A., Perrusquía, A., Al-Rubaye, S. & Guo, W. Wildfire and smoke early detection for drone applications: A light-weight deep learning approach. *Engineering Applications Of Artificial Intelligence*. **136** pp. 108977 (2024), https://www.sciencedirect.com/science/article/pii/S0952197624011357

[6] Souanef, T., Al-Rubaye, S., Tsourdos, A., Ayo, S. & Panagiotakopoulos, D. Digital Twin Development for the Airspace of the Future. *drones*. **7** (2023), https://www.mdpi.com/2504-446X/7/7/484

[7] Al-Hraishawi, H., Chougrani, H., Kisseleff, S., Lagunas, E. & Chatzinotas, S. A Survey on Non-Geostationary Satellite Systems: The Communication Perspective. *IEEE Communications Surveys And Tutorials*. **25**, 101-132 (2021,7), http://arxiv.org/abs/2107.05312%20

[8] Zeng, Y., Zhang, R. & Lim, T. Wireless communications with unmanned aerial vehicles: opportunities and challenges. *IEEE Communications Magazine*. **54**, 36-42 (2016)

[9] Al-Hourani, A., Kandeepan, S. & Lardner, S. Optimal LAP Altitude for Maximum Coverage. *IEEE Wireless Communications Letters*. **3**, 569-572 (2014)

[10] Fodor, G., Vinogradova, J., Hammarberg, P., Nagalapur, K., Qi, Z., Do, H., Blasco, R. & Baig, M. 5G new radio for automotive, rail, and air transport. *IEEE Communications Magazine*. **59**, 22-28 (2021)

[11] Whitworth, H., Al-Rubaye, S. & Tsourdos, A. Urban Air Mobility Link Budget Analysis in 5G Communication Systems. *2023 IEEE 24th International Symposium On A World Of Wireless, Mobile And Multimedia Networks (WoWMoM)*. pp. 400-406 (2023)

[12] Whitworth, H., Al-Rubaye, S., Tsourdos, A., Jiggins, J., Silverthorn, N. & Thomas, K. Aircraft to Operations Communication Analysis and Architecture for the Future Aviation Environment. *2021 IEEE/AIAA 40th Digital Avionics Systems Conference (DASC)*. pp. 1-8 (2021)

[13] Liu, X., Zhang, H., Sheng, M., Li, W., Al-Rubaye, S. & Long, K. Ultra dense satellite-enabled 6G networks: Resource optimisation and interference management. *China Communications*. **20**, 262-275 (2023)

[14] Al-Rubaye, S., Conrad, C. & Tsourdos, A. Communication Network Architecture with 6G Capabilities for Urban Air Mobility. *2024 IEEE International Conference On Consumer Electronics (ICCE)*. (2024)

[15] Al-Rubaye, S., Tsourdos, A. & Namuduri, K. Advanced Air Mobility Operation and Infrastructure for Sustainable Connected eVTOL Vehicle. *Drones*. **7** (2023), https://www.mdpi.com/2504-446X/7/5/319

[16] Tsourdos, A. 6G enabled seamless integration of satellite-terrestrial networks. *IET Conference Proceedings*. pp. 1-9(8) (2024,6), https://digital-library.theiet.org/content/conferences/10.1049/icp.2024.2226

[17] Al-Rubaye, S. & Tsourdos, A. Airport Connectivity Optimization for 5G Ultra-Dense Networks. *IEEE Transactions On Cognitive Communications And Networking*. **6**, 980-989 (2020)

[18] 3GPP "Technical Specification Group Radio Access Network; Study on New Radio (NR) to support non-terrestrial networks (Release 15). (3GPP,2020,9), Version 15.4.0

[19] Zhu, Y., Hofmann, C. & Knopp, A. Ka-Band LEO Satellite Internet of Things Channel Characterization: Survey and Measurement. *ICC 2022 - IEEE International Conference On Communications*. pp. 3076-3081 (2022)

[20] Liu, Z., Zhao, P., Guo, L., Nan, Z., Zhong, Z. & Li, J. Three-Dimensional Ray-Tracing-Based Propagation Prediction Model for Macrocellular Environment at Sub-6 GHz Frequencies. *Electronics*. **13** (2024), https://www.mdpi.com/2079-9292/13/8/1451

[21] Khuwaja, A. A survey of channel modeling for UAV communications. *IEEE Communications Surveys& Tutorials*. (2018), http://wrap.warwick.ac.uk/104438

[22] Yuan, Z. & Muntean, G. AirSlice: A Network Slicing Framework for UAV Communications. *IEEE Communications Magazine* (2020)

[23] Kelso, T. CelesTrak: Current GP Element Sets. (2024,12), https://celestrak.org/NORAD/elements/

[24] Federal Communications Commission, "LLC Request for Orbital Deployment and Operating Authority for the SpaceX Gen2 NGSO Satellite System." , https://docs.fcc.gov/public/attachments/DOC-392418A1.pdf.

[25] Al-Rubaye, S., Kadhum, E., Ni, Q. & Anpalagan, A. Industrial Internet of Things Driven by SDN Platform for Smart Grid Resiliency. *IEEE Internet Of Things Journal*. **6**, 267-277 (2019)

[26] Mohanta, K. & Al-Rubaye, S. Towards 6G Satellite-Terrestrial Networks: Analysis of Air Mobility Operations. *Electronics*. **13** (2024), https://www.mdpi.com/2079-9292/13/14/2855

[27] TSGR TS 138 214 - V15.2.0 - 5G; NR; Physical layer procedures for data (3GPP TS 38.214 version 15.2.0 Release 15). (2018), https://portal.etsi.org/TB/ETSIDeliverableStatus.aspx

https://dspace.org/

Industrial case study of aerial systems using ray-tracing and antenna optimisation

Mohanta, Krishnakanth; Al-Rubaye, Saba; Tsourdos, Antonios

2026-01-09
Institute of Electrical and Electronics Engineers (IEEE)
https://doi.org/10.1109/ccnc65079.2026.11366517
Mohanta K, Al-Rubaye S, Tsourdos A. (2026) Industrial case study of aerial systems using ray-tracing and antenna optimisation. In: Proceedings of the 2026 IEEE 23rd Consumer Communications & Networking Conference (CCNC), 9-12 Jan 2026, Las Vegas, USA

Downloaded from a DSpace repository. https://dspace.org/